

A new stereo formulation not using pixel and disparity models

Kiyoshi Oguri Yuichiro Shibata
Nagasaki University
Nagasaki, Japan

oguri,shibata@cis.nagasaki-u.ac.jp

Abstract

We introduce a new stereo formulation which does not use pixel and disparity models. Many problems in vision are treated as assigning each pixel a label. Disparities are labels for stereo. Such pixel-labeling problems are naturally represented in terms of energy minimization, where the energy function has two terms: one term penalizes solutions that inconsistent with the observed data, the other term enforces spatial smoothness. Graph cuts are one of the efficient methods for solving energy minimization. However, exact minimization of multi labeling problems can be performed by graph cuts only for the case with convex smoothness terms. In pixel-disparity formulation, convex smoothness terms do not generate well reconstructed 3D results. Thus, truncated linear or quadratic smoothness terms, etc. are used, where approximate energy minimization is necessary. In this paper, we introduce a new site-labeling formulation, where the sites are not pixels but lines in 3D space, labels are not disparities but depth numbers. For this formulation, visibility reasoning is naturally included in the energy function. In addition, this formulation allows us to use a small smoothness term, which does not affect the 3D results much. This makes the optimization step very simple, so we could develop an approximation method for graph cut itself (not for energy minimization) and a high performance GPU graph cut program. For Tsukuba stereo pair in Middlebury data set, we got the result in 5ms using GTX1080GPU, 19ms using GTX660GPU.

1. Introduction

If we define stereo as a pixel disparity labeling problem, this labeling becomes very difficult, since disparities tend to be piecewise smooth. They vary smoothly on the surface of an object, but change dramatically at object boundaries. Therefore discontinuity preserving property is necessary. The goal is to find a labeling f where f is both piecewise smooth and consistent with the observed data. This problem can be naturally formulated in terms of en-

ergy minimization. We seek the labeling f that minimizes the energy

$$E(f) = E_{data}(f) + E_{smooth}(f),$$

where E_{data} shows an energy corresponding to how the labeling f consists with the observed data, while E_{smooth} evaluates the smoothness of f . The choice of E_{smooth} is a critical issue and many different functions have been proposed [1, 3, 15]. Also, this choice requires different optimization methods [4, 5, 9, 16]. Many basic methods for stereo use scalar(1D) disparity labels. Such methods often implicitly assume front-parallel planes. For example, standard piecewise smooth(e.g. truncated linear or quadratic) pairwise regularization potentials assign higher cost to surface with larger tilt. To model surfaces more accurately Birchfield and Tomasi [2] introduced 3D-labels corresponding to arbitrary 3D planes, but this approach is limited to piecewise planar scenes. Woodford *et al.* [18] retain the scalar disparity labels while using triple-cliques to penalize 2nd derivatives of the reconstructed surface. This encourages near planar smooth disparity maps. The optimization problem is however made substantially more difficult due to the introduction of non-submodular triple interactions. Furthermore, volumetric graph cuts [17] and 3D-label energy model [14] have been proposed.

In this paper we discard pixel-disparity model which does not treat left and right image symmetrically. We treat left and right image symmetrically and introduce a novel concept of gaze lines, which are auxiliary lines defined on the cross points of rays corresponding to left and right image pixels. In our formulations, sites are gaze lines and labels are depth numbers. For this simple formulation, visibility reasoning is naturally included in the energy function, and a small smoothness term does not damage the 3D results much. Therefore, we use convex function for smoothness and visibility terms. This encourages exact optimization by graph cuts [10, 13]. Our graph structure is somewhat similar to those of [11].

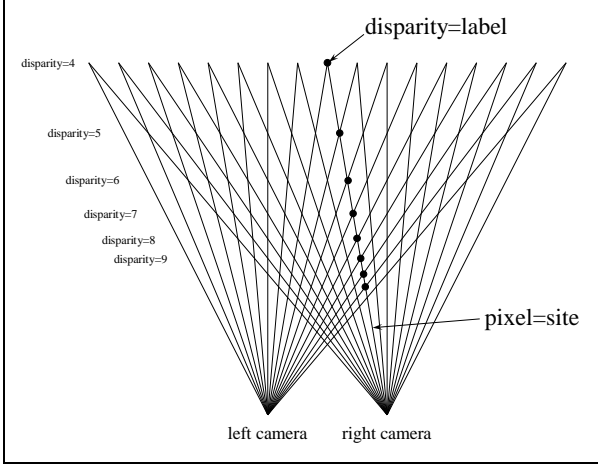


Figure 1. Conventional pixel disparity model.

2. Energy model

We define a first-order priors site-labeling problem as follows. This assigns every site v a label, which we write as X_v . The collection of all site-label assignments is denoted by X . The set of all site v is denoted by V , so $v \in V$. The set of all label l is denoted by L , so $X_v \in L$. The number of sites is n , and the number of labels is m . First order priors are defined on two-sites neighborhoods $(u, v) \in E \subset V \times V$. Here E denotes the set of all neighboring sites pairs. The energy function $E(X)$ is

$$E(X) = \sum_{v \in V} g_v(X_v) + \sum_{(u, v) \in E} h_{uv}(X_u, X_v),$$

where $g_v(X_v)$ is called data term which penalizes solutions that are inconsistent with the observed data, and $h_{uv}(X_u, X_v)$ is pairwise potential (*i.e.* interaction cost), which includes smoothness energy and visibility reasoning energy [18, 12]. We use the standard 4-connected neighborhood system. If the labels have a linear ordering and the interaction cost is an arbitrary convex function, the problem can be solved exactly with graph cuts [10]. These conditions are represented as

$$L = \{l_0, \dots, l_{m-1}\}$$

and

$$h_{uv}(l_i, l_j) = \tilde{h}_{uv}(i - j)$$

that is, labels form a line, and if

$$\tilde{h}_{uv}(i + 1) - 2\tilde{h}_{uv}(i) + \tilde{h}_{uv}(i - 1) \geq 0, \quad (1)$$

then interaction cost becomes convex function.

3. New site and label

Figure 1 shows the conventional pixel-disparity labeling, where pixels are sites and disparities are labels. Figure 2

shows ‘cross points’ of rays correspond to left and right image pixels and ‘gaze lines’ which connect some of the cross points. We denote a coordinate of a left pixel as (x_l, y_l) , a right pixel as (x_r, y_r) , here $x_l, x_r \in \{0, 1, 2, \dots, w - 1\}$, $y_l, y_r \in \{0, 1, 2, \dots, h - 1\}$. The (w, h) is image 2D size. A cross point is represented as $(x_l, x_r, y) \in \{(x_l, y_l), (x_r, y_r) | y = y_l = y_r\}$. A gaze lines is represented as $(g, y) \in \{(x_l, x_r, y) | x_r + x_l = w - 1 + 2g\}$, where g is an integer and $-w/2 < g < w/2$. A depth line is represented as $(d, y) \in \{(x_l, x_r, y) | x_r - x_l = -(w - 1) + 2d\}$, where d is an integer and $0 \leq d < w/2$. We call d a depth number. A cross point (x_l, x_r, y) is also represented as (g, d, y) by using g and d . These gaze lines form sites and depth numbers become labels.

Next we consider three cases (Figure 2). We can assign

1. the same depth numbers,
2. two depth numbers differ by one,
3. two depth numbers differ by more than one

between two neighboring sites. Assigning the same depth numbers means a front parallel plane, as same as in pixel-disparity model. Assigning depth numbers differ by one means that the two cross points are on the same ray of the right or left camera. Assigning depth numbers differ by more than one means that the cross point in the back is invisible, since it is behind some front object (Figure 3). That is, assigning labels differ by more than one to neighboring sites is inhibited in our site-labeling. Therefore, we can write

$$\tilde{h}_{uv}(i - j) = \tilde{h}_1 \times |i - j| + \tilde{h}_2 \times (|i - j| - 1) \times T(|i - j| > 1).$$

Here, i and j are depth numbers, $T(b)$ becomes 1 if b is true, otherwise 0, \tilde{h}_1 and \tilde{h}_2 are constant values, and \tilde{h}_2 is infinity (actually enough big integer). We call \tilde{h}_1 ‘penalty’ for smoothness, \tilde{h}_2 ‘inhibit’ for visibility. This $\tilde{h}_{uv}(i - j)$ satisfies Equation 1. Therefore two-sites neighboring terms become a convex function. So, we can minimize the energy by simple graph cuts. This energy function is easily mapped to the graph structure illustrated in Figure 4.

It is worthwhile noticing that Potts or truncated model is unnecessary, since any disparities change along a ray increases only once \tilde{h}_1 energy per each neighboring sites pair. It is also important that the inhibit term rejects the solutions with occlusions. In our model, invisible positions are inherently removed from the beginning. We do not seek discontinuous surface, but seek continuous surface. For dashed parts in Figure 5, we cannot know whether some objects surfaces exist or not from the only one stereo view.

Furthermore, we can think that this problem is not a sites labeling problem, but a real cross points finding problem from all cross points. Real cross points make a surface in 3D space. Graph cuts divide 3D space into two pieces by this surface. We will use the term ‘real cross point’ later.

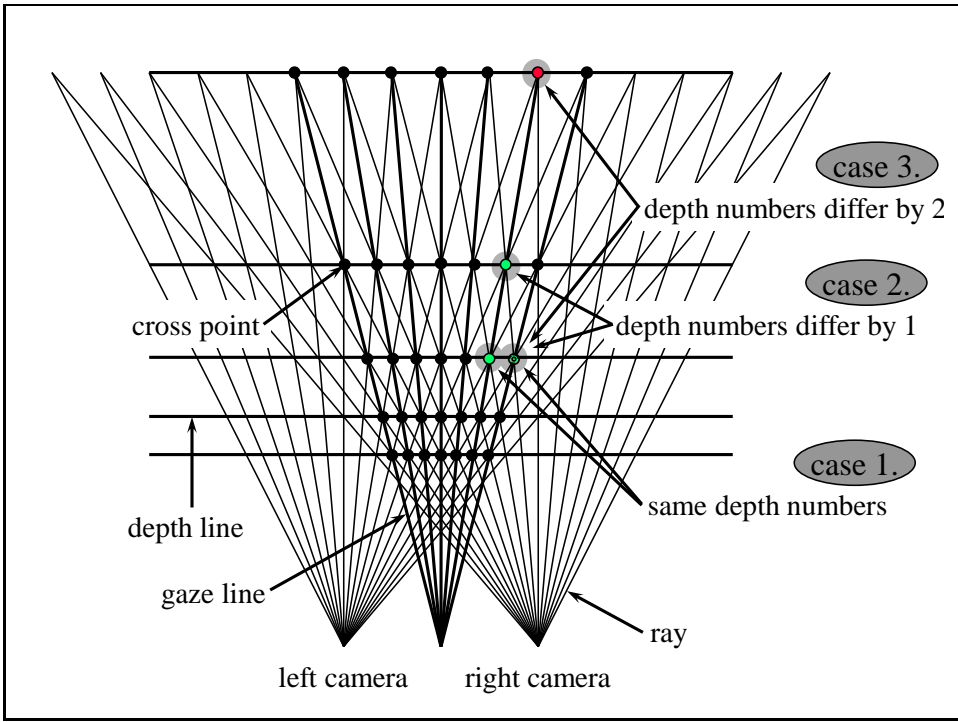


Figure 2. Our new 'gaze line' 'depth number' model. Gaze lines start the center of both eyes, *i.e.* right and left cameras. We think that I am in the center of both eyes. This figure also illustrates 'cross points'. The 'real cross points' exist on the object surface.

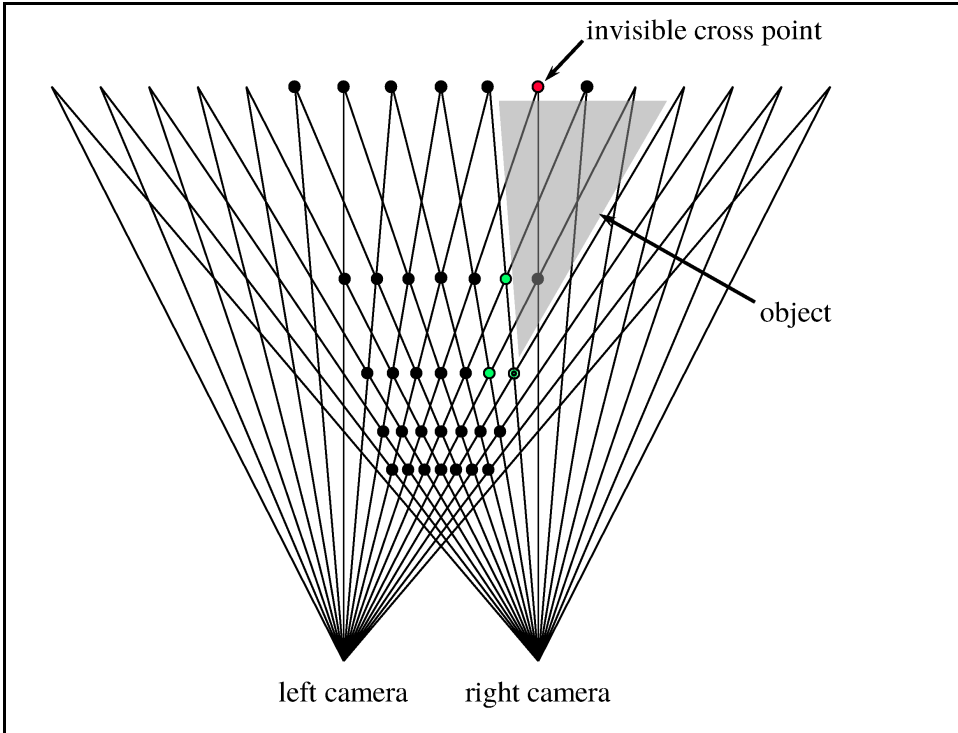


Figure 3. The posterior 'cross point' is behind some front object.

4. Experiments

4.1. Relation between disparity-model and gaze-line model

We use Tsukuba stereo pair (left: scene1.row3.col1.ppm, right: scene1.row3.col3.ppm, 384×288 pixels) and its ground truth (truedisp.row3.col3.pgm, disparity = $10 \dots 28$ pixels) in Middlebury data set. We introduce the integer coordinates (W, H, S) for cross points (g, d, y) for simplicity. W is the horizontal axis which has the left to right direction. H is the vertical axis which has the up to down direction. S is the depth axis which has the front to back direction. (W, H, S) and (g, d, y) are related as

$$\begin{aligned} W &= g + \text{offset1} \\ H &= y + \text{offset2} \\ S &= d + \text{offset3}. \end{aligned}$$

Then we denote a pixel in right image as (x, y) , and its disparity as dis . The relation between (W, H, S) and (x, y, dis) is written as follows,

$$\begin{aligned} W &= x - (lw_{\text{offset}} + rw_{\text{offset}})/2 + dis/2 \\ H &= y - h_{\text{offset}} \\ S &= (lw_{\text{offset}} - rw_{\text{offset}})/2 - dis/2 \end{aligned}$$

and

$$\begin{aligned} x &= rw_{\text{offset}} + S + W \\ y &= h_{\text{offset}} + H \\ dis &= lw_{\text{offset}} - rw_{\text{offset}} - 2S. \end{aligned}$$

Where, offset1 , offset2 , offset3 , lw_{offset} , rw_{offset} , h_{offset} define the center of cuboid area, but we omit details here. If dis changes 2, then S changes 1. Therefore in our model the half of pixels are unused. This is the weak point of our new site-labeling formulation. However, since the pixel density of CMOS camera is increasing year by year, we think this is not significant. Using this relation, we can translate each other between ground truth cross points and ground truth disparities. In dividing-by-2 operations in the above equations, we round away to get integer values.

4.2. Error count

For evaluation we define an ‘error’ as follows,

$$\text{error} = \sum_{s \in \text{all_sites}} d(s) = \sum_{d=0} d \times \text{the_number_of_such_sites}. \quad (2)$$

Here, $d(s)$ means difference between the truth depth number and the estimated depth number at site s .

d	number of such sites	percentage
0	76502	92%
1	3766	4%
2	839	1%
3	547	0%
4	98	0%
5	82	0%
6	146	0%
7	46	0%
8	36	0%
9	245	0%
10~	0	0%
error	11578	

Table 1. Breakdown of the error (Equation 2) at inhibit=1023, penalty=14. d indicates the differences to ground truth.

4.3. Graph cuts using our model

We use a cuboid area which includes $372 \times 288 \times 24$ cross points for Tsukuba stereo pair. This cuboid cross points are mapped to a graph with $372 \times 288 \times 23 + 2 = 2464130$ nodes and 19430137 edges. We use a simple sum of absolute difference data term as

$$g_v(X_v) = |L_R - R_R| + |L_G - R_G| + |L_B - R_B|,$$

where, X_v means the cross point $(g, d, y) = (x_l, x_r, y)$ in our model, therefore, (L_R, L_G, L_B) is color of left pixel (x_l, y) , (R_R, R_G, R_B) is color of right pixel (x_r, y) . The color intensity is from 0 to 255. So, $g_v(X_v)$ varies from 0 to 765. We use 1023 for the inhibit constant (\tilde{h}_2). 1023 is enough big, since increasing the inhibit constant did not increase max flow in our experiments. We do not know the theoretical reason to get the best penalty constant value (\tilde{h}_1). We sought it by experiments. Figure 6 indicates 14 is experimentally the best. At this value the error becomes 11578. Table 1 shows details of this case. The 92% of sites are equal to the ground truth. Figure 7 is the result disparity image of our stereo formulation with $\tilde{h}_1 = 14$, $\tilde{h}_2 = 1023$. Figure 6 also indicates the difference between with the inhibit constant and without it.

4.4. GPU graph cuts

This graph is successfully cut by BK Max-flow/min-cut code (maxflow-v3.01.zip at vision.csd.uwo.ca/code). It takes 3823ms at Corei7-5930K 3.5GHz CPU (Table 2). It is so slow for real time use that we have developed high speed GPU graph cuts codes. We have adopted the ‘push relabel’ algorithm with global label update [8, 6, 7]. The following is our graph_cut function described in CUDA (Compute Unified Device Architecture) for NVIDIA GPUs. Before calling this function, the ‘data’s from/to the special node S/T are translated to the positive/negative overflows

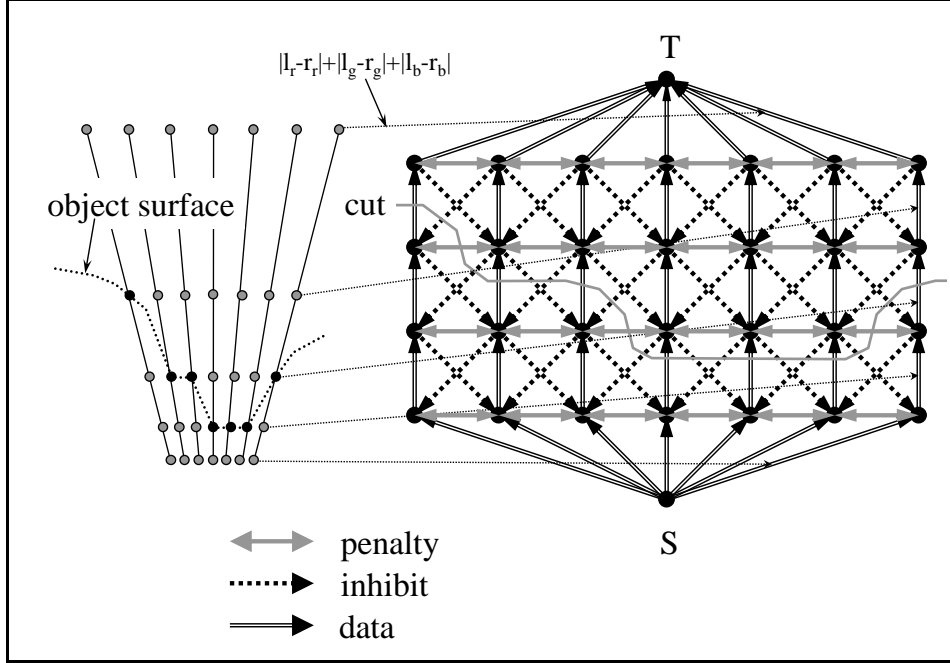


Figure 4. The graph structure representing the energy function. Left portion indicates ‘gaze lines’ and ‘depth numbers’, *i.e.* ‘cross points’, right portion indicates a corresponding graph structure. ‘Cross points’ correspond to the edges of the graph. This figure shows only one epipolar slice. Actual graph is three dimensional.

of nodes, while the ‘data’s between normal nodes are set to the edges.

```
void graph_cut(void) {
    int d;
    wave_init<<< grid, block >>>();
    for (int time = 1; time < A; time++)
        wave<<< grid, block >>>(time);
    for ( ; ; ) { // push relabel loop
        bfs_init<<< grid, block >>>();
        for ( ; ; ) {
            bfs_i<<< grid, block >>>();
            d = 0;
            bfs_o<<< grid, block >>>(d);
            if (d == 0) break;
        }
        ovf<<< grid, block >>>(d);
        if (d == 0) break;
        for (int i = 0; i < B; i++)
            push_relabel<<< grid, block >>>();
    }
}
```

Where, $grid \times block = 372 \times 288 \times 23 = 2464128$ and $\langle\langle\langle\rangle\rangle\rangle$ indicates threads invoking. Accordingly, 2464128 cuda cores in a GPU are invoked at once. Before the push relabel loop, we add the ‘wave front fetch’ operation which we have developed originally. This increases the graph cut speed twice, but we omit details here. It takes 122ms at GTX1080 GPU (Table 2). It is still slow for real time use.

4.5. Approximate graph cuts

In order to reduce the processing time, we have developed the hierarchical graph cuts which consist of two steps. In the first step, $2 \times 2 \times 2$ or $3 \times 3 \times 3$ neighboring cross points are combined into one delegate point. The first graph cut determines which delegate points include real cross points. The second graph cut finds real cross points from the all cross points which are included in a thin skin 3D area. We denote this procedure as level 1 approximation. In the expression $2 \times 2 \times 2$ or $3 \times 3 \times 3$, we call 2 or 3 as ‘block size’, $2 \times 2 \times 2$ or $3 \times 3 \times 3$ as ‘block’. These ‘block’ differ from previous block. If the block size equals to 1, the first graph cut find real cross points, that is, this means exact minimization. Using level 1 approximation, the same processing time of 14ms was achieved for both block sizes of 2 and 3 at GTX1080 GPU (Table 2). Corresponding the result disparity images are Figure 8 and Figure 9, respectively.

We have developed further approximation *i.e.* level 2 approximation. In it, the push relabel loop cuts each block separately, while the wave front fetch loop deals with the thin skin 3D area as same as in level 1. This approximation dramatically reduces the processing time. It takes only 5ms at GTX1080 GPU, 19ms at GTX660 GPU (Table 2). Corresponding the result disparity image is Figure 10. The wave front fetch algorithm is very strong in the early stage where a lots of overflows exist in the graph, but very poor for overflows to run out. Therefore this combination leads to a good result.

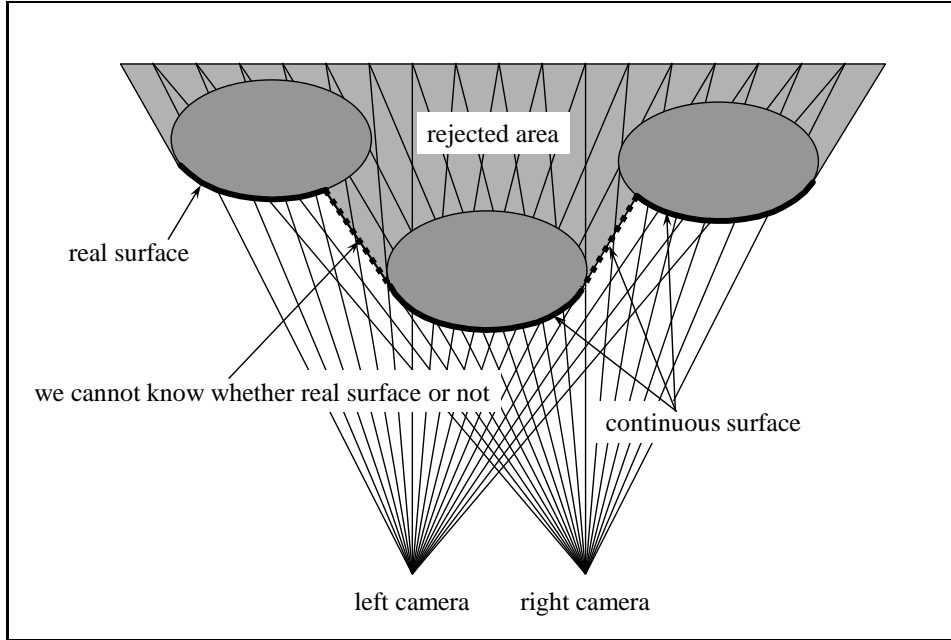


Figure 5. We seek continuous surface.

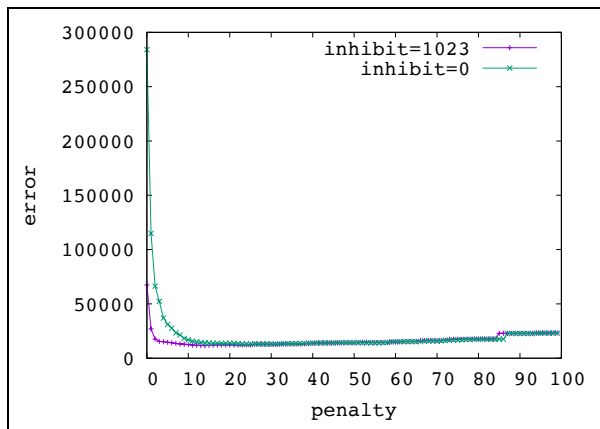


Figure 6. Relation between the penalty constant and the error (Equation 2) at the inhibit constant equals 0 and 1023.

Method	error	%	corei7	gtx1080	gtx660
BK	11578	92	3823ms	—	—
l=1 b=1	11578	92	—	122ms	472ms
l=1 b=2	14624	91	—	14ms	83ms
l=1 b=3	20657	88	—	14ms	86ms
l=2 b=3	21294	88	—	5ms	19ms

Table 2. Comparison of the errors (Equation 2) and execution times on Tsukuba. b=1 means exact minimization, l=2 indicates level 2 approximation. % indicates the sites percentage of corresponding to ground truth.

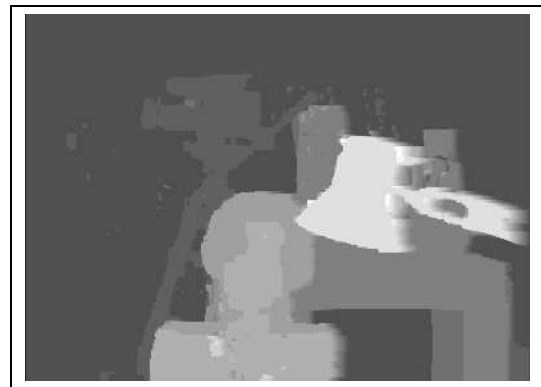


Figure 7. block_size=1, exact minimization

5. Conclusion

The new sites labeling formulation for stereo has been presented. We treat left and right image symmetrically and introduce a novel concept of gaze lines, which are auxiliary lines defined on the cross points of rays corresponding to left and right image pixels. In our formulations, sites are gaze lines and labels are depth numbers. For this symmetrical formulation, visibility reasoning is naturally included in the energy function, and a small smoothness term does not damage the 3D results much. This makes the minimization step so simple that we could develop an approximation method for graph cut itself which dramatically reduces the processing time. And now we are noticed that this symmetrical minimization could perform stereo rectification for the two cameras without any calibration objects like chess boards [19].

References

- [1] T. Ajanthan, R. Hartley, M. Salzmann, and H. Li. Iteratively reweighted graph cut for multi-label mrfs with non-convex priors. In *CVPR2015*, pages 5144–5152, 2015.
- [2] S. Birchfield and C. Tomasi. Multiway cut for stereo and motion with slanted surfaces. In *ICCV1999*, 1999.
- [3] Y. Boykov and V. Kolmogorov. An experimental comparison of min-cut/max-flow algorithms for energy minimization in vision. *IEEE Transactions on PAMI*, 26(9):1124–1137, 2004.
- [4] Y. Boykov, O. Veksler, and R. Zabih. Markov random fields with efficient approximations. In *CVPR1998*, pages 648–655, 1998.
- [5] Y. Boykov, O. Veksler, and R. Zabih. Fast approximate energy minimization via graph cuts. *IEEE Transactions on PAMI*, 23(11):1222–1239, 2001.
- [6] B. V. Cherkassky and A. V. Goldberg. On implementing push relabel method for the maximum flow problem. *Algorithmica*, 19:390–410, 1997.
- [7] A. V. Goldberg. Two-level push-relabel algorithm for the maximum flow problem. In *AAIM '09*, pages 212–225, 2009.
- [8] A. V. Goldberg and R. E. Tarjan. A new approach to the maximum flow problem. *Journal of the ACM*, 35(2):921–940, 1988.
- [9] H. Hirschmüller. Stereo processing by semi-global matching and mutual information. *IEEE Transactions on PAMI*, 30(2):328–341, 2008.
- [10] H. Ishikawa. Exact optimization for markov random fields with convex priors. *IEEE Transactions on PAMI*, 25(10):1333–1336, 2003.
- [11] H. Ishikawa and D. Geiger. Occlusions, discontinuities, and epipolar lines in stereo. In *ECCV1998*, 1998.
- [12] V. Kolmogorov and R. Zabih. Computing visual correspondence with occlusions using graph cuts. In *ICCV2001*, 2001.
- [13] V. Kolmogorov and R. Zabih. What energy functions can be minimized via graph cuts? *IEEE Transactions on PAMI*, 26(2):147–159, 2004.
- [14] C. Olsson, J. Uln, and Y. Boykov. In defense of 3d-label stereo. In *CVPR2013*, pages 1730–1737, 2013.
- [15] D. Scharstein and R. Szeliski. A taxonomy and evaluation of dense two-frame stereo correspondence algorithms. *International Journal of Computer Vision*, 47(1–3):7–42, 2002.
- [16] R. Szeliski, R. Zabih, D. Scharstein, O. Veksler, V. Kolmogorov, A. Agarwala, M. Tappen, and C. Rother. A comparative study of energy minimization methods for markov random fields with smoothness-based priors. *IEEE Transactions on PAMI*, 30(6):1068–1080, 2008.
- [17] G. Vogiatzis, P. H. S. Torr, and R. Cipolla. Multi-view stereo via volumetric graph-cuts. In *CVPR2005*, 2005.
- [18] O. J. Woodford, P. H. S. Torr, I. D. Reid, and A. W. Fitzgibbon. Global stereo reconstruction under second order smoothness priors. In *CVPR2008*, 2008.
- [19] Z. Zhang. A flexible new technique for camera calibration. *IEEE Transactions on PAMI*, 22(11):1330–1334, 2000.

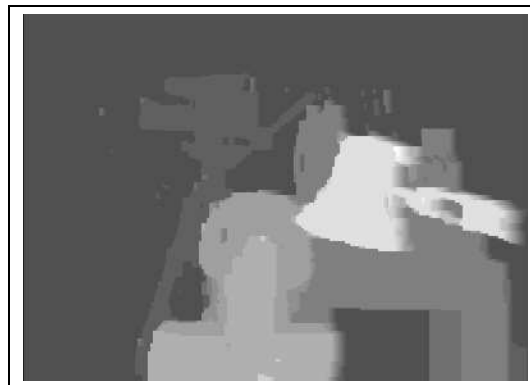


Figure 8. block_size=2, level 1 approximation

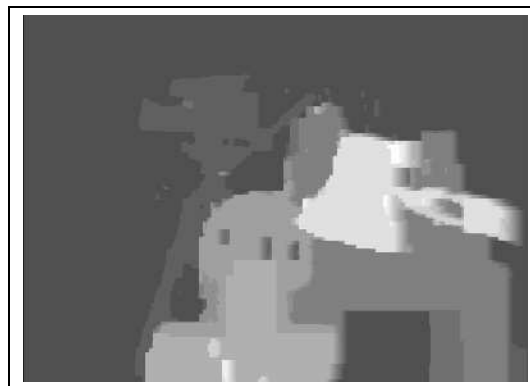


Figure 9. block_size=3, level 1 approximation

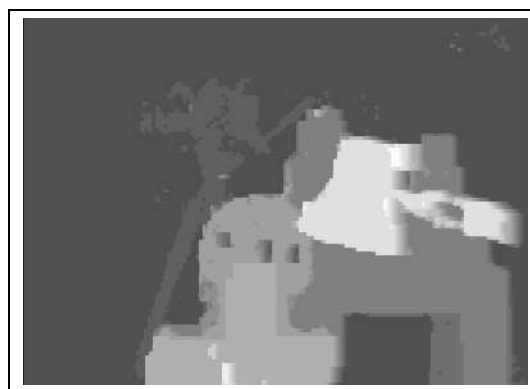


Figure 10. block_size=3, level 2 approximation